Evaluation of adhesive-free focused high-frequency PVDF copolymer transducers fabricated on spherical cavities

OPEN ACCESS
IOP Publishing
Smart Materials and Structures
Smart Mater. Struct. **29** (2020) 045026 (7pp)
https://doi.org/10.1088/1361-665X/ab7a3d

Evaluation of adhesive-free focused high-frequency PVDF copolymer transducers fabricated on spherical cavities

A Habib[1], S Wagle[2], A Decharat[1] and F Melandsø[1]

[1] Department of Physics and Technology, UiT The Arctic University of Norway, Tromsø, Norway
[2] Elop AS, Nordvikvegen 50, NO-2316 Hamar, Norway

E-mail: anowarul.habib@uit.no

Received 23 September 2019, revised 31 December 2019
Accepted for publication 26 February 2020
Published 16 March 2020

Abstract

A layer-by-layer deposition method for fabricating a focused ultrasonic transducer from piezoelectric copolymers has been developed. The fabrication process involves engraving a spherical cavity of 2 mm diameter on polyethyleneimines (PEI) polymer substrate. Surface roughness of the engraved spherical cavity is measured and compared with simulated line scan. Then, the transducer response was investigated by observing the acoustic pulse reflection from the glass plate used as reflector in a focal point. The average central frequency responses were measured to be 48.5 MHz, with a lower and upper −6 dB frequencies of approximately 25 and 76.5 MHz, yielding a bandwidth of 94.2%. A scanning hydrophone system has been employed to determine the focal zone of the transducer and compared with simulation using COMSOL Multiphysics. Two-dimensional surface scanning was performed on the test sample to provide the ultrasonic imaging of the transducer prototype and compare the image with commercial PVDF transducer with a center frequency of (48.5 ± 1) MHz.

Keywords: adhesive free, acoustic microscopy, COMSOL multiphysics, P(VDF-TrFE), polyethyleneimines

(Some figures may appear in colour only in the online journal)

1. Introduction

Scanning acoustic microscopy (SAM) is a wide field non-destructive and noninvasive technique, which has been extensively utilized for surface and sub-surface microscopic imaging of industrial objects and biological specimens during last several decades [1, 2]. The capabilities of SAM include noninvasive characterization of surface and subsurface mechanical properties of piezoelectric materials, micro-structural characterization of materials, structural health monitoring of composite structures, detection of surface defects on polymer circuit, and studies of anisotropic phonon propagations and many others [3–11].

Commercial high-frequency acoustic transducers commonly used in SAM are made from ceramic, single crystal, or thin films of piezoelectric materials. In the commercial acoustic transducers, piezoelectric material is mounted on the flat side of a buffer rod. A concave spherical sapphire lens rod is typically used to focus acoustic energy through a coupling medium (i.e. water) onto the sample plane [12]. The refractive indices of water and sapphire are 1.33 and 7.3 [13], respectively. The pronounced impedance mismatch leads to reduced sound transmissivity, significant bandwidth reduction, and geometrical aberration of the focusing beam [6].

In order to overcome the aforementioned shortcomings, Lockwood *et al* [14] and Smolorz and Grill [6] demonstrated a different way of transducer fabrication. In [6, 14], a flexible polyvinylidene fluoride (PVDF) piezoelectric polymer film

was attached to a spherical epoxy surface. Focused copolymer transducers with a film thickness of around 6.0 μm on aluminum substrates have been reported in [15, 16]. Michelle *et al* have reported a P(VDF-TrFE) focused transducer with an operating frequency of over 40 MHz and approximately a 75% bandwidth [16]. Moreover, a focused P(VDF-TrFE) copolymer transducers with 5.0 μm thick film on copper substrate [17] showed central frequency of 110 MHz. This value is significantly higher than that obtained in [15, 16]. Here, most of the studies showed $\lambda/4$ resonance mode with the heavy backing material. Our previous studies of unfocused transducer on polyethyleneimine (PEI) substrate showed a resonance frequency at $\sim\lambda/2$ which is higher than $\lambda/4$ resonance mode [18]. Ferroelectric PVDF and its copolymer PVDF trifluoroethylene P(VDF-TrFE) are widely used to make ultrasonic sensors and transducers [16–29]. The application of P(VDF-TrFE) piezoelectric copolymer has been broadened from hydrophone fabrication to ultrasonic imaging and further to photoacoustic imaging of the microstructures of tissue, dermatology, ophthalmology, and biomicroscopy imaging [18, 24, 29–33]. These polymer-based transducers (PVDF refractive index = 1.43) provide much better acoustic matching with commonly used materials like water, human tissues and have outstanding broadband receiving performance for a small scanning area [16]. Powder or pellet-like PVDF copolymer materials are flexible to some extent and relatively easy to process. These polymers are suitable for achieving high frequency operation with a large bandwidth for ultrasonic sensors and transducers [18, 24, 29, 31–33].

Nonconducting epoxy is used as a baking material for fabricating the PVDF high-frequency transducers. However, to fabricate it as a curved surface is rather challenging. Some works employed pre-poled flexible piezoelectric polymer film to fabricate focusing transducers on a curved aperture where additional adhesive layers are required [6, 16, 17]. The additional epoxy layers may contribute to an increased inhomogeneity (e.g. through-thickness variation) and high surface roughness. Also, they hinder the propagation of ultrasound wave [6]. There are several other methods to fabricate PVDF and its copolymer transducers. These include spin coating, hot pressing, stamping, and spraying on a flat substrate [16, 17, 19–22, 34]. There have also been attempts to develop adhesive-free spin coating process on spherical aperture or alternate approach of pressing pre-polarized film on high impedance conductive silver epoxy backing substrate using stainless steel spheres with heat treatment of short duration to make focusing transducers [17]. However, these fabrication processes require special equipment and complicated fabrication process.

The motivation of the present work is to demonstrate a new approach of fabricating high-frequency P(VDF-TrFE) focusing transducer by employing adhesive-free layer-by-layer deposition technique. The main aim of the current work is to build and characterize the prototype for adhesive-free high-frequency ultrasonic focusing transducers using spherical cavities in PEI to focus acoustic energy. PEI has been selected as the focusing lens material for several reasons, such as good thermal stability, good impedance match to the PVDF copolymer, and low acoustic attenuation [35]. The deposition of P(VDF-TrFE) copolymer on the PEI substrate is an adhesive-free method. The present process does not introduce any additional layer. It only creates a bond between the involved materials, namely the lens material PEI and sputtered electrode of P(VDF-TrFE). The main advantages of our process are following: (i) it eliminates the problems imposed by additional adhesive layers, (ii) it presents lower the impedance mismatch between the lens material and the electrode (iii) it presents decreased attenuation as compared to other techniques.

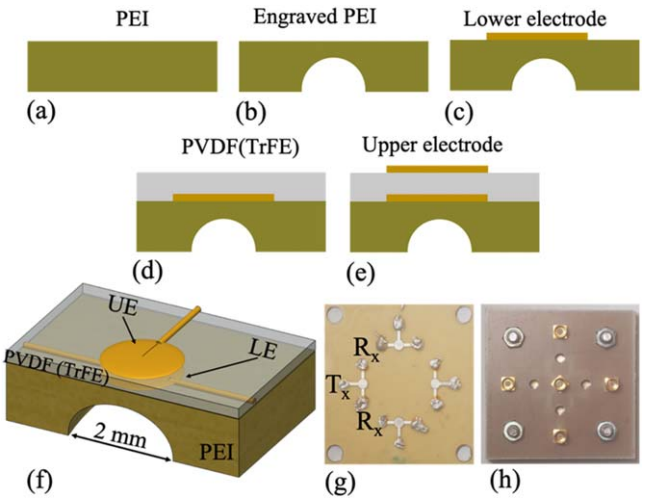

Figure 1. A schematic diagram illustrating the involved steps for fabricating the P(VDF-TrFE) copolymer transducer. The process starts with a PEI polymer backing substrate (a) which is engraved by milling spherical cavities with a 2.0 mm diameter, partially into the material (b). The top of the substrate is then pre-treated and sputtered through a mask to yield an 80 nm thick patterned Au layer (c) acting as the lower electrode (LE). A P(VDF-TrFE) layer is then spin coated onto this electrode (d), degassed under vacuum and thereafter annealed at 130 °C. Finally, an upper electrode (UE) was sputtered on the top of P(VDF-TrFE) by repeating the process used for the lower electrode (e), which completes the fabrication. A 3D illustration of the prototype transducer is also shown in (f) together with optical image (g) and (h) of a transducer panel containing 4 transducers. Here (g) and (h) image the upper side of the panel before and after it was connected to a PCB used for further cable connection.

2. Transducer fabrication

The fabrication process begins by engraving the four spherical cavities of 2 mm diameter in PEI polymer substrate of a dimension of 30 × 30 × 0.85 mm^3 (width, length, thickness) using a milling drill. The tip of the four spherical cavities are drilled up to 0.65 mm to make spherical cavities as shown in figure 1.

The cavities are cleaned with acetone and ethanol after milling to remove unwanted material and grease. Then, a plasma cleaner is used to increase the wettability of the substrate. This is followed by sputtering a thin layer of gold ~80 nm on the flat side of the substrate pointing away from

the cavity. The sputtering is performed through a high-resolution metal mask to form the first electrode (lower) layer. After that, fluid-phase P(VDF-TrFE) (77:23 molar ratio) dissolved in appropriate amount of solvent is spin-coated on top of the patterned electrode. The spin-coated substrate is then degassed under 1 mbar atmosphere pressure to vaporize the solvent, and thereafter annealed at a temperature of 130° C for 8 h to increase the crystallinity. The annealed film thus obtained has a thickness around 12 μm. Finally, upper electrode with a gold target was deposited on the top of P(VDF-TrFE) with the patterned metal mask of thicknesses ~80 nm, which completes the fabrication. An image of the focusing transducer panel with 4 circular apertures and 12 connection points is shown in figure 1(g). For each aperture, one electrode line is used as a sender T_x and two electrode lines denoted as R_x serve as receivers. In order to obtain a reliable electrical connection to the lower electrode, the PVDF layer was removed by using a solvent. Then, a very small layer of conductive epoxy was coated on top of all 12 connecting points to enhance the conductivity.

For poling and characterize the acoustic response, each of the transducers in the substrate were connected directly onto a printed circuit board (PCB) using small spring contacts as shown in figure 1(h) in order to minimize additional inductive and capacities effects caused by open connectors. In order to make the P(VDF-TrFE) layers piezoelectric, they were polarized at room temperature by connecting a high voltage AC source to the lower electrodes, while the upper ones were grounded.

3. Transducer characterization

In order to confirm the engraved spherical cavity surface roughness, a line scans (300 and 400 μm in length) with a nano-profiler have been performed inside the cavity of the particular transducer [36].

In the line scan, inside the cavity of the PEI, there is small variation observed in comparison with simulated line scan in figure 2. The root mean square (rms) values for the 300 and 400 μm scans were determined to 0.8 and 1.04 μm, respectively. These variations relate to the surface roughness of engraving PEI, which occurs due to the use of drill head for making the spherical cavity on PEI. Surface roughness within the cavity also plays a vital role in the propagation of acoustic wave in the medium. Major height variations originate during the engraving of PEI and act as particle-like defects. They can significantly alter the acoustic wave intensity and orientation. The ultrasonic signal strength decays during its propagation through such material because of scattering from these rough surfaces. Scatters much smaller than the wavelength can be modelled by Rayleigh scattering which is proportional to the third power of the grain size and fourth power of the frequency. The wavelength of the corresponding to (48.5 ± 1) MHz is (31 ± 2) μm. The determined wavelength (31 ± 2) μm which is comparable with the surface roughness of the engraving PEI. Such small variation of the roughness will not affect the propagation wave of the transducer.

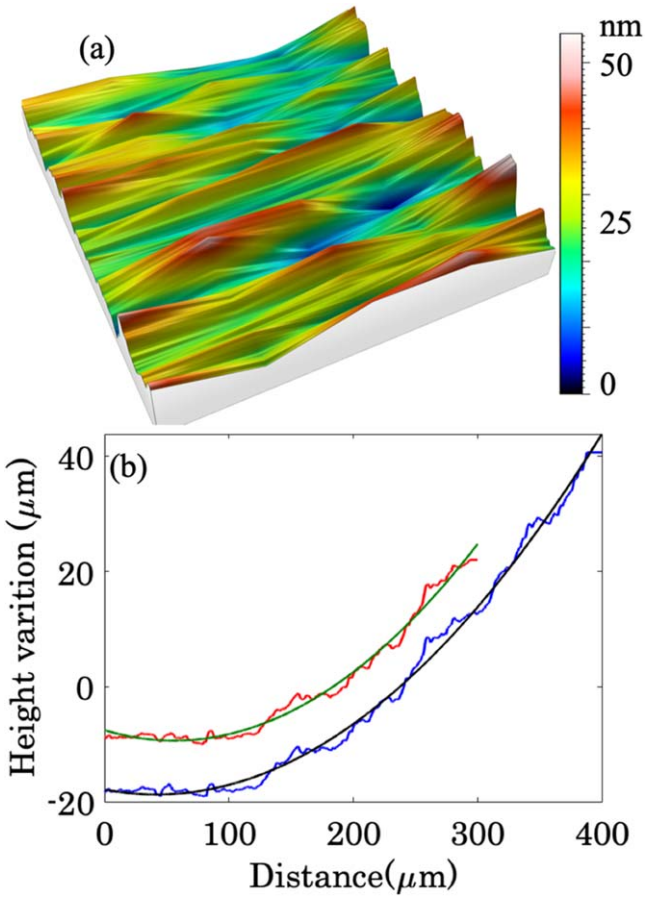

Figure 2. 3D surface profile on the P(VDF-TrFE) active area (a) using a nano-profiler and scanning area was 200 × 200 μm^2, maximum height variation was 50 nm. The thickness distribution over the active (2.5 mm) was quite uniform that is visible from the surface profile. Figure (b), surface profile on a spherical cavity within the PEI substrate. Scan length is 300 and 400 μm in two different places within the cavity. The experimental results were also fitted with simulated line scan.

Therefore, the defect scattering becomes significant if the surface roughness exceeds one-hundredth of the wavelength. From figure 2, it is evident that the surface roughness of the cavity is negligible compared to the excited acoustic wave. Therefore, the defect scattering becomes significant if the surface roughness exceeds one-hundredth of the wavelength.

4. Experimental procedure

To characterize the transducer prototype, we have used various methods including numerical modelling, hydrophone pressure measurement in an acoustic scanning tank, reflective pulse characterization, and imaging of test samples. The results obtained from these methods will be described in the following sections.

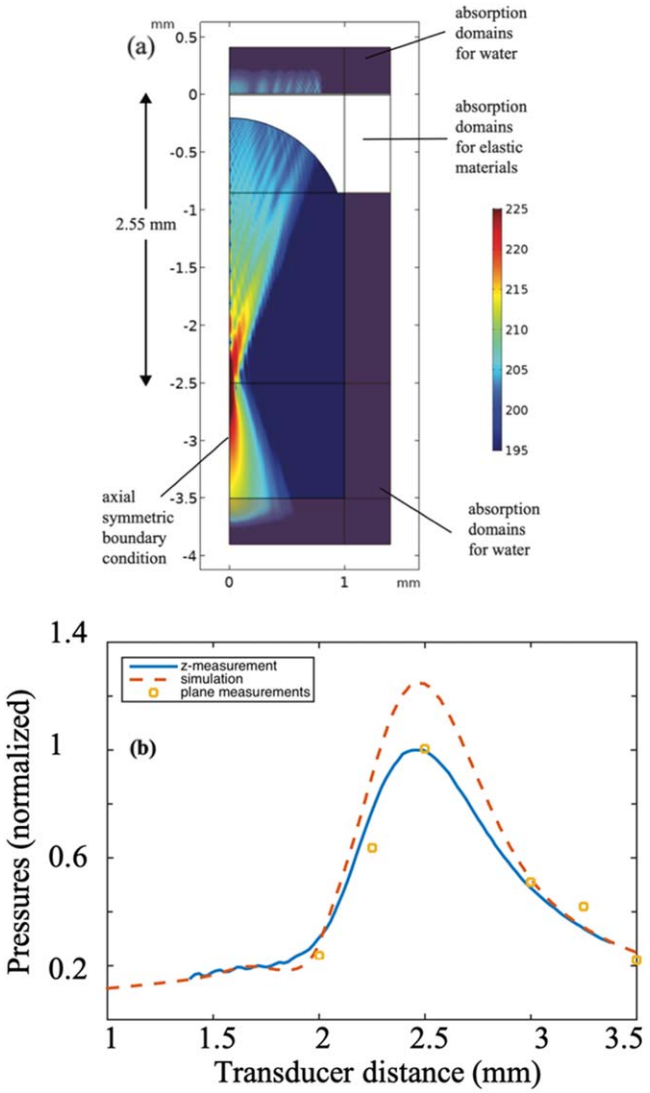

Figure 3. (a) Acoustical field distributions in water at 45 MHz frequency obtained from COMSOL for the focusing transducer. All the absorption domains for COMSOL modeling are marked in the figure (a). (b) Dependence of acoustical amplitude with respect to the lateral displacement of glass reflector. Here, the dashed line represents acoustical amplitude obtained from COMSOL. Both results were normalized with the acoustical amplitude at the focal point.

4.1. Numerical modelling and hydrophone measurements of pressure fields

The physical geometry of the proposed transducer was implemented in COMSOL Multiphysics and modeled both in the time- and frequency-domain. An example of the pressure amplitude field generated from a frequency computation with a 45 MHz driving frequency, is shown in figure 3(a). Here the polymer PEI was implemented as linear isotropic elastic materials while P(VDF-TrFE) was model as piezoelectric and electrostatic domain in the COMSOL terminology.

For both materials some attenuation was included using a Rayleigh damping model to resemble physical values around 0.01 and 0.1 for the wave attenuation coefficients in PEI and P(VDF-TrFE), respectively. The Rayleigh damping model which includes the two parameters α and β, was chosen since it can easily be extended to time-domain modelling. The drawback, on the other hand, is that the model cannot exactly describe a loss that is proportional to frequency (denoted as the linear loss model), which are the case in many materials. However, by fitting the α and β parameters to a condition where the Rayleigh model equals the linear loss model at two frequencies one each side of the transducer band, the Rayleigh model can be used as a good approximation. This approach was therefore chosen to fit the two damping models at frequencies 25 and 75 MHz yielding a good match to the linear loss model within the transducer band.

From figure 3(a) one notice that the pressure generated from the transducer is only shown in the domains containing water. This is because water is modelled as an isotropic fluid denoted as 'pressure acoustics' in COMSOL, providing the pressure as a solution variable. The pressure amplitude field given in a decibel scale in the figure, indicated a focal distance around 2.5 mm away from the surface of the piezoelectric film which is defined as position $z = 0$ in the figure. This focal distance agrees quite well with a focal distance 2.55 mm estimated from using ray tracing and Snell's law on the PEI-water interface, assuming a planar wavefield excited from the transducer.

To simulate infinite large water domains above and under the transducer, we have used so-called absorption domains around the computational domain. The purpose of these domains is to attenuate the outgoing waves in such a way that the reflected wave fields induced internally in the domain and from the other boundaries, become small. COMSOL has several options for absorbing fields or simulating infinite large domains, including boundary conditions that give low reflections under various conditions, and build-in absorbing domains like perfectly matched layer (PML). Several of these methods very tested out for the current model, and found to work well under some conditions. However, for the used software version (5.2 A), we were not able to find obtain good general solutions that worked both for time and frequency modelling, using the build-in domain and boundary methods. We have therefore used a customized absorption model were the attenuation is gradually increase from an inner value η_i (also used as the internal damping) at the domain entrance at position s_i to a larger value η_o at the outer boundary s_o. The attenuation η within the domain is then assumed to follow a quadratic functionality $\eta(s) = \eta_i + \gamma(s - s_i)^2$ where $\gamma = (\eta_o - \eta_i)/(s_o - s_i)^2$. For the elastic domains, absorbing boundaries for PEI and P(VDF-TrFE) were implemented by using this approach on both the α and β parameters in the Rayleigh attenuation model. For the water domains, it was found sufficient to use a single parameter model with the bulk viscosity as the attenuation parameter. Similar to the elastic domains, this parameter was also gradually turn on from zero following the quadratic relation. For both the elastic and fluid domains it was necessary to adjust the outer parameter values η_i as well as the size of the absorption domains given by $(s_o - s_i)$, in order to optimize the absorption method. Our customized method was also compared to PML for frequency computations, and found to give comparable results.

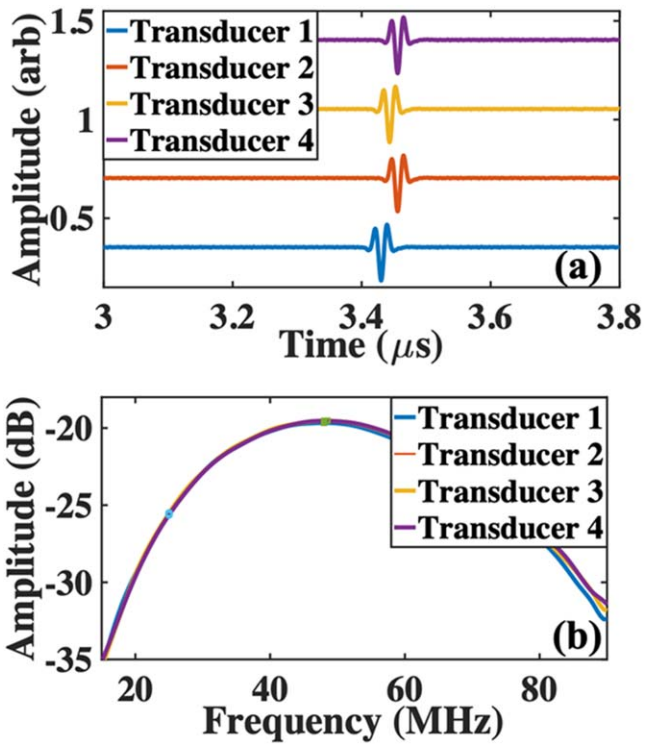

Figure 4. Measured reflections for the four transducers in the panel shown in the time domain (a). The reflections were obtained by putting a glass plate at a focal point (2.5 mm). The corresponding amplitude spectra (b) shown in dB with average center frequencies (48.5 ± 1 MHz) and the lower −6 dB cut-off frequencies given by the green and blue squares, respectively.

In addition to modelling the transducer in COMSOL, we have also measured the transducer pressure using a hydrophone. Both the hydrophone and the transducer were inserted in a water tank, where the pressure in an arbitrary position in the front of the transducer could be measured using a 3D actuator system. Figure 3(b) show the measure pressure field along the z-axis together with the axial field obtained from COMSOL. The reflection from a glass plate was recorded at the focal distance in water, which is also considered as backing material in the experiment. Table 1 summarizes the specification of the fabricated transducer being used to perform all the experiments.

4.2. Acoustic pulse reflection measurements

Figure 4 represents the acoustic reflection of the focused transducers (4 transducers) from the glass plate at a focal point using the setup described in [24, 29]. The frequency response has been estimated as the ratio between the output and input power from the glass reflector. The average central frequency of the four transducers were measured to be (48.5 ± 1) MHz, with a lower and upper −6 dB frequencies of approximately 25 and 76.5 MHz, yielding a bandwidth of 94.2%. Several factors may influence the measured acoustic responses, such as bandwidth limitation in the current amplifier, wave effects (e.g. diffraction and attenuation), surface roughness of PVDF and PEI, and the spherical cavity surface roughness.

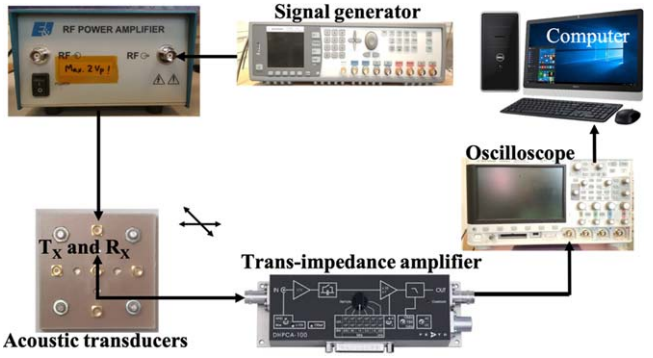

Figure 5. Instruments and components used in the experimental setup for imaging a selected area of a Norwegian one-Krone coin as a test object. As the driver excitation pulse for the image test, a Ricker wavelet (second derivate of a Gaussian signal) with 5 V peak to peak amplitude was used.

4.3. Acoustic imaging of test sample

In order to explore the advantages of the fabricated transducers, acoustic imaging was performed on metallic Norwegian 1 Krone coin. An experimental setup for acoustic imaging of a test sample is shown in figure 5. The experimental setup consists of an arbitrary wave generator (Agilent 81150A) and a voltage amplifier on the sender side. A current amplifier acting as a trans-impedance amplifier (FEMTO DHPCA-100) on receiver side and a digital oscilloscope (Agilent 3024A) and the water bath with scanning arm (precision acoustic) [37].

For acoustic imaging, the element of the transducer was excited with a second derivative of Gaussian signal in the signal generator with 5 V peak to peak. This signal was sent into the voltage amplifier to amplify the signal and then sent to the upper electrode of the transducers from one side i.e. T_x as shown in figure 1(g). This excites waveforms into the PEI lens material through the coupling media water and to the sample. The acoustical reflections caused by the transmitted signal on the surface of the sample was picked up as currents on the lower electrodes R_x and sent to the trans-impedance current amplifier. This amplifier converts the current into an output potential. This potential signal was then sampled by a digital oscilloscope, which is capable of digitizing with up to 12 bit accuracy in high resolution.

The sample was scanned in the x and y direction with 25 μm step length for acoustic imaging by focusing acoustic energy on the top surface of coin. Figure 6(a) shows the optical images of the Norwegian 1 Krone coin while figure 6(b) shows zoomed view of highlighted scanned area. The acoustical image obtained from the experiment is shown in figure 6(c). The image shows detailed patterns of the coin structures and exhibits the capability of fabricated transducer in high frequency imaging.

The lack of previous publications that reports physical tests for transducer similar to ours have made it very difficult to perform the comparison. We have therefore only been able to meet these comparisons partially by relating our work to the following papers which all are related in terms of used PVDF polymer for transducer. Smolorz *et al* have imaged a

Table 1. Fabricated transducers summary.

Electrode thickness	PVDF thickness	PEI thickness	Cavity diameter	Focal length	Central frequency
80 nm	12 μm	850 μm	2 mm	2.55 mm	48.5 MHz

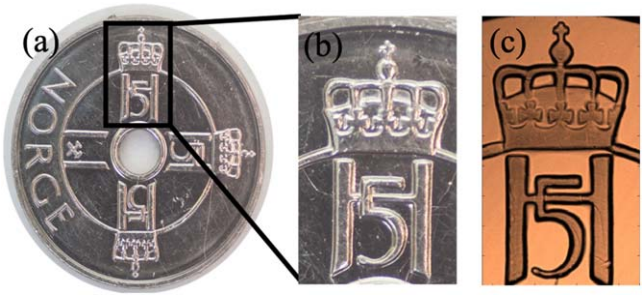

Figure 6. Optical image of the Norwegian 1 Krone (a)–(c) acoustic image of the Norwegian 1 Krone of the same area using prototype transducer. Image size is 7 × 5 mm^2 and step size is 25 μm in both directions. The center frequency of the transducer was set to 48.5 MHz. The transducer was focused on the coin surface, and the voltage amplitudes from the received echo were plotted for each step, to create a 2D image.

transistor by employing a PVDF transducer [6]. The fabricated transducer reported a small ultrasound amplitude in acoustic imaging. The main reason for less ultrasound amplitude is to use a conductive epoxy as an intermediate layer, in the same time it also led to high surface roughness in the fabricated transducer. Kim *et al* have fabricated a dual frequency P(VDF-TrFE) transducer for an adjustable harmonic imaging [38]. This dual frequency transducer is capable to detect clear harmonic content of the scattered signal from the microbubbles especially in the range of 6–12 MHz. Sanat *et al* developed a prototype roller ultrasonic scanning system for concrete inspection using a piezoelectric PVDF array transducer operating in separate transmission and receiver modus [39]. Such roller scanning system is capable of imaging a large concrete area with relatively short inspection time with a higher penetration depth. Han *et al* validated an experiment of an acoustic lens based focusing idea for ultrasound imaging that eliminates synthetic aperture focusing typically used in conventional US imaging systems [40]. Sanat *et al* also presented surface damage imaging on flexible circuits of using a high frequency P(VDF-TrFE) polymer focused transducer [18]. The 2D scanning showed very detailed surface variations with the expected resolution, with defects in the solder mask clearly visible in acoustic scanning images. Skoglund *et al* have developed a 3D PVDF based ultrasonic scanner which can be employed in a wide range of application such as different layers in a laminate structure, impact damage, boreholes etc [41].

5. Conclusion

The present study shows that it is possible to fabricate a reliable PVDF copolymer focusing transducers using an adhesive-free layer-by-layer deposition method by engraving milled spherical cavies in a PEI polymer substrate. The proposed method processes P(VDF-TrFE) in its fluid phase, thus making it adhesive-free in the sense that it does not require any additional adhesive layers for material binding. The transducer was acoustically. characterized by pulse/echo ultrasonic measurements and compare with FEM models. In this study, the center frequency of the four transducers were estimated to (48.5 ± 1) MHz with 94.2% bandwidth for 12 μm thickness film. Additionally, two-dimensional surface scanning was performed on the test sample in order to demonstrate the capability of the transducer prototype in acoustic imaging.

Acknowledgments

This work was supported by The Research Council of Norway through the project 'Subsea sensors'.

ORCID iDs

A Habib https://orcid.org/0000-0001-6515-3145
A Decharat https://orcid.org/0000-0002-9545-6646

References

[1] Korpel A, Kessler L and Palermo P 1971 *Nature* **232** 110
[2] Zimmerman M C, Harten R D Jr, Shieh S-J, Meunier A and Katz J L 2019 *Biomechanical Systems* (Boca Raton, FL: CRC Press) pp 105–38
[3] Habib A, Shelke A, Vogel M, Pietsch U, Jiang X and Kundu T 2012 *Ultrasonics* **52** 989–95
[4] Habib A, Shelke A, Vogel M, Brand S, Jiang X, Pietsch U, Banerjee S and Kundu T 2015 *Acta Acust. United Acust.* **101** 675–83
[5] Lee Y C 2001 *Japan. J. Appl. Phys.* **40** 359
[6] Smolorz S and Grill W 1996 *Res. Nondestruct. Eval.* **7** 195–201
[7] Hofmann M, Pflanzer R, Habib A, Shelke A, Bereiter-Hahn J, Bernd A, Kaufmann R, Sader R and Kippenberger S 2016 *Transl. Oncol.* **9** 179–83
[8] Merks E J W, Bouakaz A, Bom N, Lancee C T, Van Der Steen A F W and De Jong N 2006 *IEEE Trans. Ultrason. Ferroelectr. Freq. Control* **53** 1730–8
[9] Wagle S, Habib A and Melandsø F 2017 *Japan. J. Appl. Phys.* **56** 07JC05
[10] Guzmán E, Cugnoni J and Gmür T 2015 *Smart Mater. Struct.* **24** 055017
[11] Brown L F and Mason J L 1996 *IEEE Trans. Ultrason. Ferroelectr. Freq. Control* **43** 560–8
[12] Zou W, Holland S, Kim K Y and Sachse W 2003 *Ultrasonics* **41** 157–61

[13] Sutilov V A 2013 *Physik des Ultraschalls: Grundlagen.* (Berlin: Springer)
[14] Lockwood G, Ryan L, Hunt J and Foster F 1991 *Ultrasound Med. Biol.* **17** 653–66
[15] Kimura K and Ohigashi H 1986 *Japan. J. Appl. Phys.* **25** 383
[16] Robert M, Molingou G, Snook K, Cannata J and Shung K K 2004 *J. Appl. Phys.* **96** 252–6
[17] Jeong J S and Shung K K 2013 *Ultrasonics* **53** 455–8
[18] Wagle S, Decharat A, Habib A, Ahluwalia B S and Melandsø F 2016 *Japan. J. Appl. Phys.* **55** 07KE11
[19] Kimura K and Ohigashi H 1987 *J. Appl. Phys.* **61** 4749–54
[20] Brown L F and Carlson D L 1989 *IEEE Trans. Ultrason. Ferroelectr. Freq. Control* **36** 313–8
[21] Brown L, Carlson R and Sempsrott J 1997 *Proc. IEEE Ultrasonics Symp. 1997* pp 1725–7
[22] Decharat A, Wagle S and Melandsø F 2013 *Proc. Euro. Freq. and Time Forum & Int. Freq. Cont. Symp. 2013* pp 266–9
[23] Chung C-H and Lee Y-C 2010 *NDT E Int.* **43** 96–105
[24] Decharat A, Wagle S and Melandsø F 2014 *Japan. J. Appl. Phys.* **53** 05HB16
[25] Rathod V, Mahapatra D R, Jain A and Gayathri A 2010 *Sensors Actuators* A **163** 164–71
[26] Wagle S, Decharat A, Bodö P and Melandsø F 2013 *Appl. Phys. Lett.* **103** 262902
[27] Kim H-J, Lee H and Ziaie B 2007 *Biomed. Microdevices* **9** 83–90
[28] Korai Y and Baba A 2012 *Japan. J. Appl. Phys.* **51** 07GC03
[29] Melandsø F, Wagle S, Decharat A, Habib A and Ahluwalia B S 2016 *Japan. J. Appl. Phys.* **55** 07KB07
[30] Daeichin V, Chen C, Ding Q, Wu M, Beurskens R, Springeling G, Noothout E, Verweij M D, van Dongen K W and Bosch J G 2016 *Ultrasound Med. Biol.* **42** 1239–43
[31] Bloomfield P E, Lo W-J and Lewin P A 2000 *IEEE Trans. Ultrason. Ferroelectr. Freq. Control* **47** 1397–405
[32] Chae M-K, Kim M-J, Ha K-L and Lee C-B 2003 *Japan. J. Appl. Phys.* **42** 3091
[33] Xi L, Li X and Jiang H 2012 *Appl. Phys. Lett.* **101** 173702
[34] Decharat A, Wagle S, Habib A, Jacobsen S and Melandsø F 2018 *Smart Mater. Struct.* **27** 025001
[35] Fukuhara M 2003 *J. Appl. Polym. Sci.* **90** 759–64
[36] https://kla-tencor.com/Surface-Profiling/p7.html
[37] https://acoustics.co.uk/product/ums-tank-specification/
[38] Kim J, Lindsey B D, Li S, Dayton P A and Jiang X 2017 *Proc. SPIE* **10170** 101700T
[39] Wagle S, Chapagain K R, Bjerke W, Melandsø T and Melandsø F 2017 *Proc. 15th APCNDT Conf.* ID 248
[40] Chinni B *et al* 2016 *Proc. SPIE* **9708** 97081Q
[41] Skoglund E, Salberg A-B and Baarstad T 2015 Google Patents